CHAPTER-III

MATERIALS AND METHODS

Chapter-III
MATERIALS AND METHODS

This chapter includes a detailed description of the various methods and techniques used to accomplish the research objectives. It deals with the collection of the materials, preparation of the samples, chemicals used for the analysis, experimental design for the process standardization, preparation of the powder, quality attributes, and their storage study during storage under different conditions.

3.1 Materials and Methods

3.1.1 Raw material

Ripe pineapples were purchased from the local market of Tezpur, Assam, India. Their selection was based on the uniformity of the yellow-green color of the pineapple. The samples were thoroughly cleaned with water to eliminate dirt and other extrinsic matters. The external surfaces were wiped with a dry cloth, cut into small pieces, and ground in a kitchen mixture grinder (Model # 2663, Usha, India) to obtain smooth pineapple pulp.

3.1.2 Chemicals

Skim milk powder (SMP), used as a foaming agent, is manufactured by Amul, India, and has a protein content of 35%. The carboxymethyl cellulose (CMC) fixed at a level of 0.25% was used as a foam stabilizer, and starch at a fixed quantity of 1% was used as a drying aid. The CMC and starch were procured from Merck, Tezpur, India.

3.1.3 Equipment and Instruments

Many instruments were used in the present study to successfully carry out the experimental work and reach the research objectives. A list of the instruments, their make and models, along with the purpose, is listed in Table 3.1.

3.1.4 Preparation of sample

Pineapples of good quality were brought from the local area of Tezpur University, Tezpur, Assam, India. The pineapples were washed, cleaned, and cut into pieces. The Pineapple pieces were ground to produce the pulp using a home mixer grinder (Model: 2663, Usha, India), which was further passed through the sieve to obtain homogeneous, smooth pulp. The pulp was then stored at a refrigeration temperature of 4 °C until further use.

Table 3.1 List of equipment with make and model used in the study

No's	Equipment's	Make and model	Purpose
1.	Weighing Balance	Model: UW1020H Make: Shimadzu Corporation, Japan	To measure the weight of samples and chemicals
2.	pH Meter	Model: pH510 Make: Eutech Instruments	To measure the pH of samples and buffers.
3.	Magnetic Stirrer	Model: JS1199/4 Make: Jain Scientific Works, India	To continuously stir and mix samples
4.	Water Bath	Model: BW-20G Make: JEIO Tech, Korea	To provide a hot water bath
5.	Refractometer	Model: 0-32 Make: Erma, Tokyo	To measure TSS in terms of °Brix
6.	Hunter Colour Lab	Model: UltraScan VIS Make: Hunter Lab, USA	To measure the color properties of the sample
7.	Refrigerated centrifuge	Model: 3-18 K Make: SCIQUIP	To separate different particles from solutions under refrigeration.
8.	Food processor	Model: 2663 Make: Usha	To mix and grind samples
9.	Rheometer	Model: MCR 72 Make: Anton Par	To study the flow behaviour of samples.
10.	Tray dryer	Model: NE-12 Make: Newtech Equipment, Mumbai	To study the drying behaviour of the samples.
11.	Vacuum Oven	Model: OV-11 Make: JEIO TECH	To measure the moisture content of the sample under vacuum conditions
12.	UV-Vis Spectrophotometer	Model: CE7400 Make: Cecil Instruments Limited, Uk	To measure the absorbance of the samples
13.	Kjeldhal machine	Model: ELITE-EX Make: Pelican Equipment	To measure the crude protein content of the samples
14.	Gas pycnometer	Model: PYC-100A Make: Porous Materials, Inc	To measure the true density of the samples
15.	Refrigerated centrifuge	Model: 3-18 K Make: SCIQUIP	To separate different particles from solutions under refrigerated conditions
16.	Humidity chamber	Model: MES-117A Make: Matrix Eco Solutions Pvt. Ltd	To maintain the samples with a particular humidity

3.1.5 Cold plasma treatment

Plasma treatments of pineapple pulp were carried out in a Dielectric Barrier Discharge (DBD) Plasma chamber comprised of a plasma generator (Zeonics System and Aerospace Pvt. Ltd., India). For the DBD treatment, pineapple pulp samples were poured into a glass

Petri plate while maintaining a thickness varying from 2, 3, and 4 mm. The Petri plates were then placed between two parallel plate attachment chambers connected with an electrode on the top of the parallel plate. The gap between the plate and the treatment chamber was fixed at 15 mm, as shown in Fig. 3.2. Plasma treatments were then employed in a DBD plasma chamber with varying voltages from 15, 20, 25 kV and treatment times of 3, 6, 9, 12, and 15 min. These voltage and treatment times were fixed based on the previous experimental trials, which may not develop any oxidation of juice components, discolorations, or flavour degradation. All the tests were repeated thrice, and their enzymatic activity (PPO and POD) and physicochemical properties were measured.

3.1.6 Enzyme activity measurement

3.1.6.1 Crude enzyme extraction

The enzyme extraction solution was made by following the methods of Terefe et al. (2010). For the Stock solution, added 0.2 M SSP buffer (pH 6.5) with 4% (W/V) polyvinyl polypyrolidone (PVPP), Triton X-100 (1 % (V/V)), and 1M NaCl. 1M NaCl was added to the extraction solutions to enhance the extraction rate of enzymes from the pulp sample. The stock solution was then stored at a refrigeration temperature of 4 ^{o}C and used as an extraction solution for further use.

A work plan is to study the plasma pre-treatment effects on the characteristics of pineapple pulp, such as enzyme inactivation, foam stabilization, and kinetic modelling. The Work plan to fulfil the objective #1 is provided in Fig. 3.1.

The extracted solution was mixed with the pineapple pulp at a 1:1 ratio to extract crude enzymes. The mixed solution was then homogenized and centrifuged at 10,000×g (Refrigerated centrifuge, Velocity 14R, Dynamica) for 30 min at 4 ^{o}C. The centrifuged solution was used to measure the activity of the enzymes in CP-treated pineapple pulp. All the chemicals used in this study were purchased from Sigma Aldrich and are of high analytical grade.

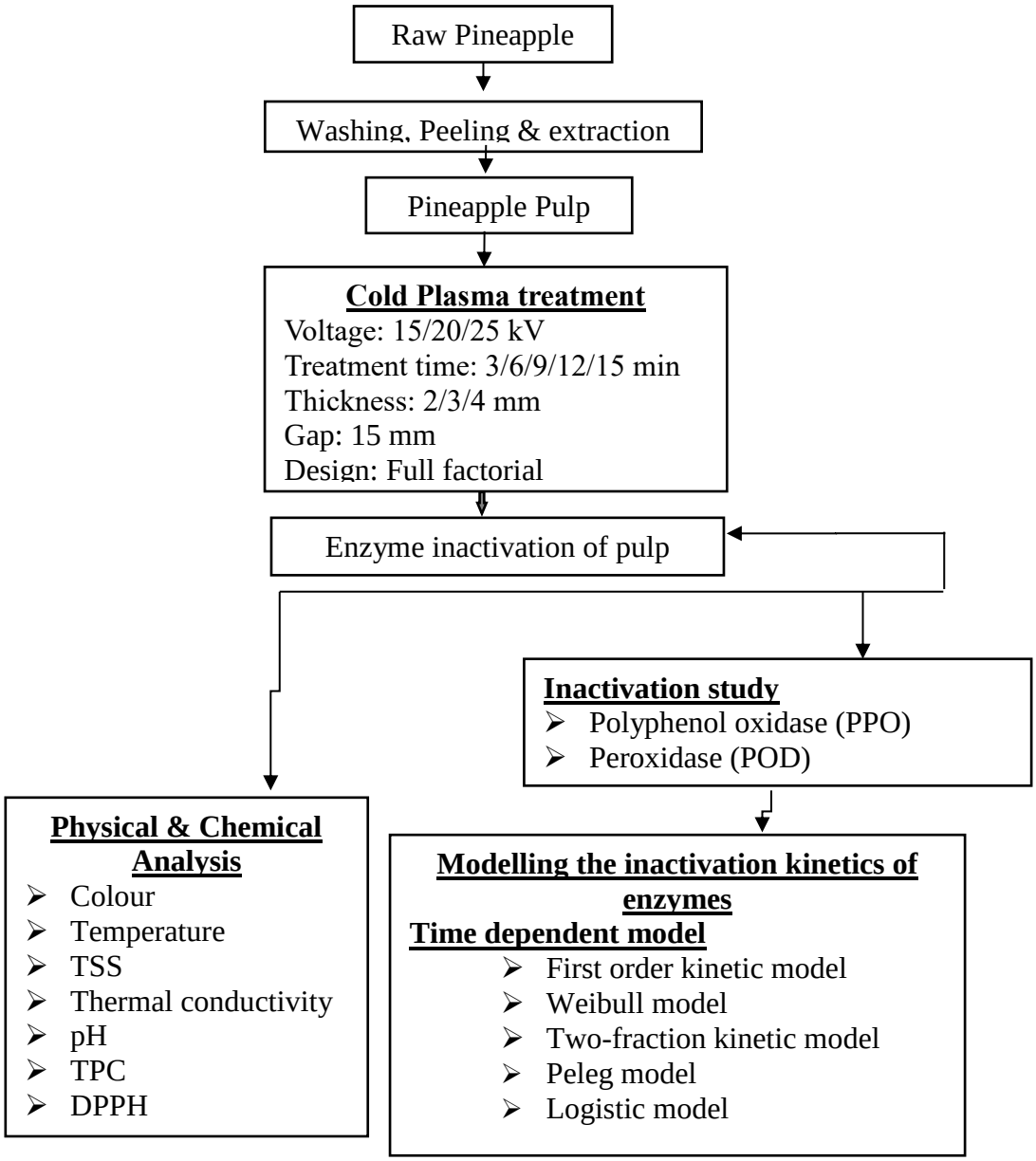

Figure 3.1 Work plan flowchart of objective # 1

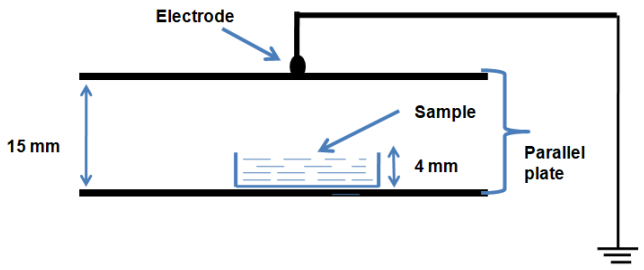

Figure 3.2 Cold Plasma Parallel plate attachments

3.1.6.2 PPO and POD activity

The activity of PPO and POD in pineapple pulp was analyzed using the methods reported by Terefe et al. (2010). For PPO enzyme activity, 0.15 M pyro-catechol was prepared in SSP of pH 6.5. Enzyme extract containing 200 µl was then added to 2 ml of pyro-catechol. Immediately after adding the catechol solution, sample absorbance was taken in a spectrophotometer (UV-VIS Double Beam Spectrophotometer, Halo DB-20S, Dynamica) at 420 nm for 5 min at every 10 s in kinetic mode.

The enzyme extract containing 200 µl was added with 1.5 ml of 0.05 M SSP buffer for POD enzyme activity. For the substrate reaction, the same hydrogen peroxide solution and pyrogallol concentration were added to the buffer solution. After adding the reactant solution, the assay was immediately taken at 485 nm for 5 min in a kinetic mode. The change in absorbance/min/mL of the fresh sample was used to measure the enzyme assay. A blank solution for the enzyme estimation was made with an SSP buffer. The entire assay was freshly prepared, and its activity was measured in triplicate.

3.1.7 Mathematical modelling of enzymes

Enzymatic browning in Fruits and vegetables is problematic due to various oxidative enzymes in pineapples, viz., Polyphenol oxidase (PPO), peroxidase (POD), and protease. When fruits and vegetables containing these enzymes are exposed to atmospheric air, they may cause undesirable changes due to enzymatic browning. Enzymatic browning causes nutritional and colour loss and may degrade the overall food quality. The application of both conventional and non-conventional treatments may reduce enzymatic browning. In the present study, non-thermal Dielectric Barrier Discharge (DBD) plasma was applied with varying treatment-time combinations, and their activities were estimated. Further, a few mathematical models were examined to check the adequacy of data, and their predicted parameters were used to depict their efficacy.

The relative activities of enzymes under various processing conditions were fitted with different mathematical models to study the enzyme degradation kinetics [Illera et al., (2019); Terefe et al., (2010)]. The rates of inactivation of enzymes under treatments were determined from the model coefficients. Relative activity is the enzyme activity under

different treatment conditions with respect to its original activity, which was determined from Eq. 3.1.

Times of treatment with respect to the relative activity of enzymes were fitted with various mathematical models to estimate the model's coefficients and their fitness.

$$RA = \frac{A_t}{A_0} \qquad \text{Eq. (3.1)}$$

Where RA is the relative activity of enzymes, A_o and A_t are the activity at treatment, t=0 and t' min, respectively, and k is the rate constant.

3.1.8 Mathematical models

3.1.8.1 First-order model

Times of treatment with respect to relative activities of enzymes were fitted with (eq. 3.2) to predict the model parameters and test the model's fitness in enzyme inactivation.

$$\frac{A_t}{A_0} = \exp(-k_F t) \qquad \text{Eq. (3.2)}$$

k_F is the rate constant of the model equations, and 't' is the treatment time

3.1.8.2 Weibull model

The Weibull model (Eq. 3.3) was fitted with the experimental RA versus time data to study the degradation of enzymes with the cold plasma treatment time in pineapple pulp (llera et al., 2019).

$$log_{10}\left(\frac{A_t}{A_0}\right) = -\mathrm{bt^n} \qquad \text{Eq. (3.3)}$$

b is the Weibull nonlinear parameter, n is the shape factor, and 't' is the treatment time

3.1.8.3 Two-fraction kinetic model

Two-fraction kinetics models were fitted with residual enzyme data to investigate several isoenzymes, i.e., the labile and stable enzymes in the cold plasma-treated pineapple pulp. Both enzymes were independently estimated using the first-order kinetic model (Brochier et al., 2016).

$$RA = A_L \exp(-k_L t) + A_S \exp(-k_S t) \qquad \text{Eq. (3.4)}$$

A_L and A_S are the liability and stability factors for the two-fraction kinetic model, and k_L and k_S are the rate constants for the liability and stability factors in (min^{-1}), respectively.

3.1.8.4 Peleg model

The experimental RA versus time plot was fitted with the Peleg model (eq. 3.5) to study the enzyme degradation with time in cold plasma-treated pineapple pulp (Planinic et al., 2005).

$$RA = 1 \pm \frac{t}{K_1 + K_{2.}.\, t} \qquad \text{Eq. (3.5)}$$

Peleg's model parameters K_1 and K_2 are the initial rate and capacity constant, respectively.

3.1.8.5 Logistic model

A three-parameter Logistic model, Eq. (3.6), has been proposed to study the kinetic modelling of enzymes in cold plasma-treated pineapple pulp.

$$RA = \frac{100 - A_{min}}{1 + \left(\frac{t}{t_{50}}\right)^{p}} + A_{min} \qquad \text{Eq. (3.6)}$$

Where A_{min} (≥0) is the minimum value attained by the logistic function, t_{50} is the time necessary to reach half of their maximal activity, and p is the power factor.

3.1.9 Physical & Chemical Analysis

3.1.9.1 Colour

The colour values of the control pineapple pulp and the pulp after the DBD plasma treatment at room temperature were measured using a Hunter Lab Colorimeter (USA). Colour values were measured in terms of L*(lightness), a*(redness), and b*(blueness). Total colour change (**Δ**E), chroma (C*), and Hue (H*) of the pulp samples were determined from the L*, a*, and b* values by using Eqs. 3.7, 3.8, and 3.9, respectively.

$$\boldsymbol{\Delta E} = \sqrt{(\boldsymbol{L^*_{control}} - \boldsymbol{L^*_{treated}})^2 + (\boldsymbol{a^*_{control}} - \boldsymbol{a^*_{treated}})^2 + (\boldsymbol{b^*_{control}} - \boldsymbol{b^*_{treated}})^2} \qquad \text{Eq. (3.7)}$$

$$\boldsymbol{C^*} = \sqrt{\boldsymbol{a^{*2}} + \boldsymbol{b^{*2}}} \qquad \text{Eq. (3.8)}$$

$$\boldsymbol{H^*} = \boldsymbol{tan^{-1}}\left(\frac{\boldsymbol{a^*}}{\boldsymbol{b^*}}\right) \qquad \text{Eq. (3.9)}$$

3.1.9.2 Total phenolic content (TPC)

The TPC of the samples was determined using the methodology described by Hossain and Rahman (2011) with minor modifications. Approximately 5 ml of extraction solution was mixed with the same volume of the pineapple pulp and then centrifuged (Refrigerated centrifuge, Velocity 14R, Dynamica) for 10 min at 10000 rpm at 4 ^{o}C temperature. The collected centrifuged solution was then used as an extraction solution for the TPC estimation. For the TPC estimation, about 0.5 mg of extract was taken with 2.5 ml of 10% Folin-cobalt reagent and shaken vigorously until adequately mixed. After 4 min, 1 ml of 15% Na_2CO_3 was added by keeping the solution at room temperature for 2 hr. Absorbance was measured by performing the UV-VIS spectrophotometer (UV-VIS Double Beam Spectrophotometer, Halo DB-20S, Dynamica) at 760 nm. TPC was calculated in terms of µg Gallic acid equivalents (GAE)/ml of fruit juice.

3.1.9.3 DPPH scavenging activity

The DPPH activity was determined based on the scavenging effect of the DPPH free radical by following the methods discussed by Islam et al. (2019). For extraction, 1 mL of pineapple juice was mixed with 1 mL of a methanol–water solution (7:3, v/v) and centrifuged at 5000 rpm for 20 min. A 0.1 mL aliquot was taken from the supernatant and mixed with 1.9 mL of methanol, followed by the addition of 2 mL of 0.1 mM DPPH solution prepared in methanol. The mixture was vortexed and incubated in the dark at room temperature for 30 min, after which the absorbance was measured at 517 nm using a UV–Vis spectrophotometer (AQUAMATE 8100, Thermo Fisher Scientific, USA).

3.1.9.4 pH and conductivity

pH and conductivity were measured using a pH meter and a conductivity meter, as mentioned in Table 3.1.

3.1.10 Statistical analysis of the model parameters

A full factorial design was used to design the experiment with varying DBD voltages (15-25 kV), (3-level) treatment time (3-15 min), (5-level), and sample depth (2-4 mm) at three levels. MATLAB software was used to fit the various kinetic models, and the efficacies of the models were estimated in terms of R^2 and root mean square error (RMSE) (Kreyenschmidt et al.,2009; Zhou et al.,2012). All the treatments were repeated thrice, and

their mean significant difference was estimated using the Tukey HSD Test at $p<0.05$. PCA analysis was also conducted to determine the relationship between the kinetic parameters in Minitab Statistical Software (Version 20.0).

3.1.11 Model validation

Model validation is carried out to examine whether the output of the predicted models agrees with the experimental observations while fulfilling the statistical criteria. The performance of the fitted models was estimated in terms of the accuracy (A_f) and bias (B_f) factors. The accuracy factor (A_f) implied that the models were well predicted with the observations (A_f value close to 1 implies minor variances). At the same time, B_f signifies how the observed values deviated from the fitted line. The A_f value close to 1 provides the best-fitted models, while the B_f value near equality shows less deviation of predicted models from the actual observations. The factors (A_f and B_f) were determined using the Eqs. 3.10 and 3.11(Valdramidis et al., 2007).

$$\text{Accuracy factor}(A_f) = 10^{\sum_{i=1}^{n}\left(\frac{\left|\log\left(\frac{\text{estimated(esi))}}{\text{observed(obi)}}\right)\right|}{n}\right)} \quad \text{Eq. (3.10)}$$

$$Biasfactor\left(B_f\right) = 10^{\sum_{i=1}^{n}\left(\frac{\left\{log\left(\frac{estimated(esi))}{observed(obi)}\right)\right\}}{n}\right)} \quad \text{Eq. (3.11)}$$

For selecting the best model suitable for the enzymes, AIC and BIC were considered for assessing the highest accuracy and comparing the suitability of the models in the present context. The AIC and BICs were estimated using the Eqs. 3.12 and 3.13 are presented below (Akaike, 1973; Stoica & Selen, 2004).

$$AIC = -2\left(-\frac{n}{2}ln\sigma^2\right) + 2p \quad \text{Eq. (3.12)}$$

$$BIC = -2ln\left(-\frac{n}{2}ln\sigma^2\right) + plnn \quad \text{Eq. (3.13)}$$

Where σ^2, p, and n are the variance, number of model constants, and number of observations, respectively.

3.1.12 Foaming of pineapple pulp based on product characteristics

The foaming of pineapple pulp and its foaming and powder characteristics were carried out as per objective#2. The detailed work plan for objective 2 is provided in Fig. 3.3.

3.1.12.1 Pineapple pulp foam preparation

The washed ripe pineapples were peeled and cut into pieces to extract the smooth pulp using a mixer grinder (Model: 2663, Usha, India). The smooth pulp was adjusted to 10 °Brix by a refractometer and then whipped with skimmed milk powder (SMP), carboxymethyl cellulose (CMC), and starch. The cold plasma electric field treatment was optimized based on the maximum inactivation of enzymes (PPO and POD) in pineapple. The smooth pineapple pulp was treated under optimized conditions. The treated pulp was then whipped by adding skimmed milk powder (SMP) at 2, 4, and 6% w/w concentrations and whipped for 60, 90, and 120 s. The sodium salt of CMC [0.25% (w/w)] and starch [1% (w/w)] were added at a fixed concentration as a foam stabilizer and drying aid, respectively.

3.1.12.2 Experimental Design

The pineapple pulp was subjected to cold plasma treatment under fixed (25 kV for 15 min) conditions as optimized from objective 1. The full factorial experiment was designed to experiment with two independent parameters, and 9 experiments with triplicate runs were obtained. The input variables selected were SMP concentrations [2-6% (w/w)] and whipping time [60-120 s]. Various foaming experiments were conducted to obtain the combination of the optimal input variables that may result in the best foam formation. Foaming behaviour (expansion volume, foam density, foam stability, drainage volume, and drying time) and rheological parameters (storage modulus, loss modulus, complex viscosity, phase angle, and yield stress) were considered as the responses for the statistical analysis.

3.1.13 Foaming behaviour

3.1.13.1 Expansion volume (EV)

The expansion volume (EV) is the percentage increase in foam volume with respect to its initial volume. It is expressed in % and can be determined using Eq. (3.14), as shown below (Kadam & Balasubramanian, 2011).

$$EV(\%) = \frac{V - V_o}{V_o} \times 100 \qquad \text{Eq. (3.14)}$$

V_0 and V are the initial and final (cm^3) pulp and foam volumes, respectively.

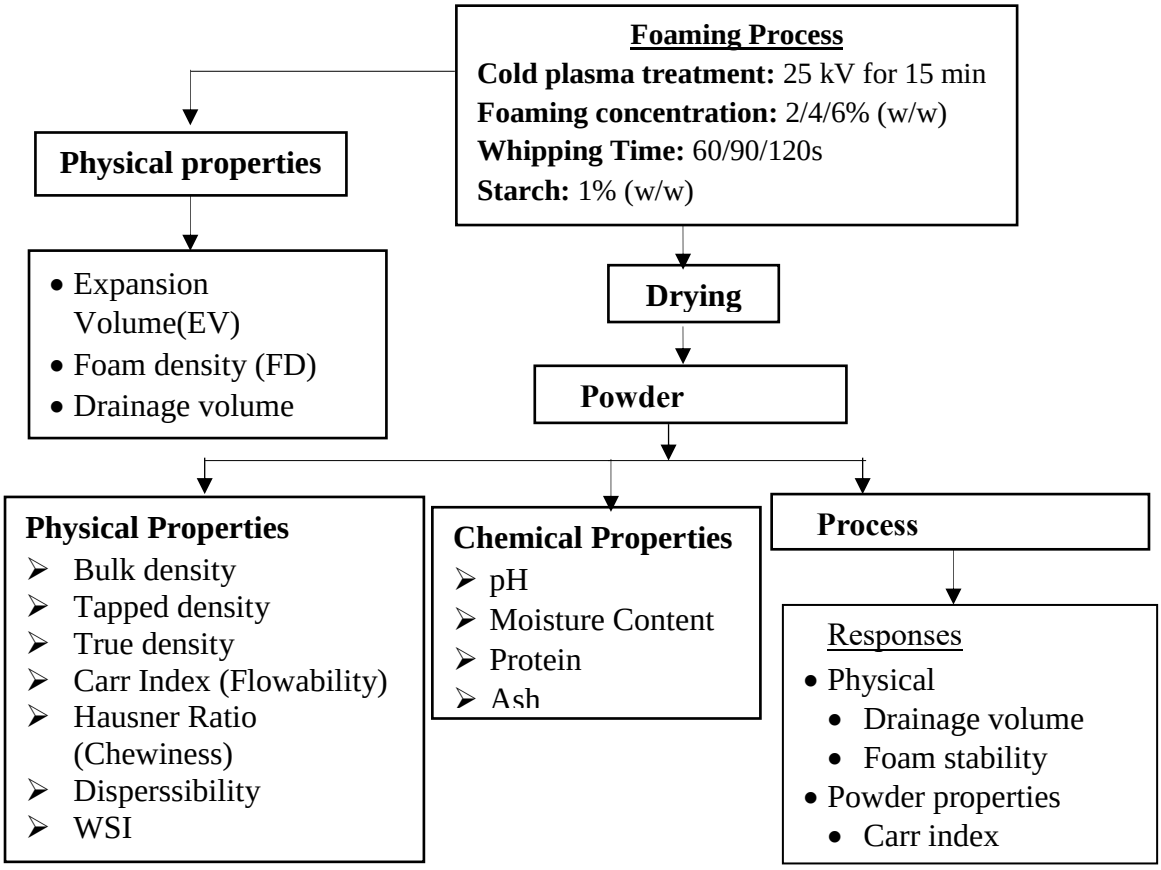

Figure 3.3 Work plan flowchart of objective # 2

3.1.13.2 Foam density (FD)

About 50 mL of whipped foam was taken for foam FD without collapsing the structure, and its corresponding foam weight was noted (Asokapandian et al., 2016). The pineapple pulp foam density was measured in kg-m^{-3}using Eq. (3.15).

$$\mathrm{FD}(\mathrm{kg.\,m^{-3}}) = \frac{\text{Weight of foam}}{\text{The volume of foam}} \qquad \text{Eq. (3.15)}$$

3.1.13.3 Drainage volume (DV) and foam stability (FS)

The foam drainage was used to test the foam lamella strength in terms of drained liquid volume over time, while stability measures the foam's ability to hold the developed air-liquid interface of the foam. Both parameters have an inverse relationship, and lower DV gives higher FS. For both measurements, around 50 mL of foam was kept at rest for 1 h, and the drained liquid volume (mL) was measured after 30 s (LVS) and 1 h (LVM) (Chang & Chen, 2000). The difference in their volume is the foam's drainage volume, and the ratio gives stability, as shown in (Eqs . 3.16 and 3.17).

$$\text{DV (mL)} = \text{LVM} - \text{LVS} \qquad \text{Eq. (3.16)}$$

$$\text{FS}(\%) = \frac{\text{LVM}}{\text{LVS}} x100 \qquad \text{Eq. (3.17)}$$

3.1.14 Foam mat drying of pulp

After the foam formation, the whipped foam was poured on a pre-weighed Petri plate, maintaining a sample thickness of 10 mm, and dried at a temperature of 60 °C (NE-12, Newtech Equipment, Mumbai, India). The weight loss of each sample with an interval of 30 min was recorded. The time taken to reach 0.06 g of moisture/g of dry solid moisture content was selected as the drying time of the final foam mat dried powder.

3.1.14.1 Drying models

The moisture ratio data have been fitted with the two empirical drying model equations (Eqs. 3.18, 3.19, and 3.20) to predict the model kinetics parameter of the foam mat dried PPF (Diamante et al., 2010).

Page Model,	$\text{MR} = \exp(-\text{kt}^{\text{n}})$	Eq.(3.18)
Henderson and Pabis' model,	$\text{MR} = \text{a}\exp(-\text{kt})$	Eq.(3.19)
Wang and Singh ,	$\text{MR}=1+(\text{at})+(\text{bt}^2)$	Eq.(3.20)

A, b, k, and n were the empirical model coefficients, and MR was the moisture ratio.

3.1.15 Quality attributes of powder

The quality attributes of powder were bulk density, porosity, rehydration ratio, flowability, dispersibility, and solubility. The bulk density (ρ_b) was measured by following the methods discussed in the literature by Asokapandian et al. (2016). Approximately 10 g of powder sample was taken into a measuring cylinder for bulk density. The volume and mass of powder were noted; the mass divided by volume gave the untapped bulk density. The samples were tapped gently 10 times, and corresponding volumes were noted; the obtained values were reported as tapped bulk density. Six samples were tested each time.

Particle density (ρ_d) (kg/m³) of powder was analyzed by taking around 5 g of powder sample and pouring 10 mL of petroleum ether into it. The sample was entirely suspended in the solution by continuously shaking it and reading the volume increase. The ratio of the powder taken in g to the volume of powder suspended (mL) with petroleum ether (PE)

subtracted from the amount of PE used gives the particle density (Jinapong et al., 2008). The porosity or void fraction (ε) of the powder bed was determined from the bulk density and particle density of a powder using Eq. (3.21) (Jinapong et al., 2008).

$$\varepsilon(\%) = \frac{\rho_d - \rho_b}{\rho_d} \qquad \text{Eq.(3.21)}$$

Carr index (CI) and Hausner ratio (HR) were determined to measure the flowability and cohesiveness of the powder samples, respectively, as described by Jinapong et al. (2008). The flowability and cohesiveness were selected based on the ranges of CI and HR, respectively.

Dispersibility is the speed with which the powder forms lumps and agglomerates that fall apart when reconstituted with water (Jinapong et al., 2008). For dispersibility of the powder, approximately 5 g of the sample was taken with 50 mL of distilled water, maintaining a temperature of 25℃. The sample was forcefully agitated for 15 seconds, moving back and forth 25 times over the beaker's diameter. A 100-mesh sieve was then used to pour the reconstituted powder into Petri dishes that had been previously weighed. The sieved sample was then dried at 105 ℃ until a constant mass was reached (Bhusari et al., 2014), and dispersibility was calculated using Eq. (3.22).

$$Dispersibility(\%) = \frac{[(W + a) \times S_p]}{(a \times S)} \qquad \text{Eq. (3.22)}$$

Here, a is the amount of pineapple powder, W is the mass of water used for reconstitution, S_p is the percentage of total solids present in the powder, and S is the percentage of sieved dry matter.

The solubility of powder measures the final condition of the powder constituents interacting with water. WAI and WSI were measured following the methods explained by Grabowski et al. (2006). Approximately 2g of powder was taken with 25 mL of distilled water in a pre-weighed 50 mL centrifuge tube and stirred continuously with a glass rod. The solution was allowed to rest for 30 min in a water bath to maintain a temperature of 30 ^{o}C. The solution was then centrifuged for 10 min at 8000 rpm, and the supernatants were dried for 10 h in a vacuum oven at 70 ^{o}C. The WAI of the powder is the ratio of the mass of the dry solid to

the total solid present in the sample. The WSI of powder was the ratio of the dry solid that remained after centrifugation and the total mass of dry matter in the original sample; it was expressed on a percent basis. Four samples were examined each time for WAI and WSI.

3.1.16 Chemical properties

The protein and total ash content of the powder were estimated using the standard methods described by AOAC (1999). For ash determination, crucibles were dried at 105 °C for 30 min, cooled in a desiccator, and weighed. 1g of finely ground sample was placed in the pre-weighed crucible and incinerated in a muffle furnace at 600 °C for 6 h. After that, the crucible containing ash is cooled, and the weight is taken. The ash content was expressed as the ratio of the weight of ash to the weight of the original sample.

3.1.17 Statistics and interrelation

The analysis concerning the rheological models was carried out employing MATLAB software. Rheological parameters with the highest R^2 and lowest RMSE were judged as the best-fit model. Tukey HSD (IBM SPSS 23.0) test is done to check the mean differences in the samples with varying independent variables at a $p<0.05$ significance level. Partial component analysis (PCA) using Minitab Statistical Software (Version 20.0) was used to identify the inter-relationship among the independent and dependent parameters of the rheological, foaming, and powder properties. Pearson correlation coefficients were also determined to identify the interaction between/among variables. A design expert was used to standardize the parameters' effects on foaming.

3.1.18 Effect of selected additives on the physical and rheological properties of foam

Foaming conditions for foam mat drying were standardized as per the objective. 2, and their quality parameters were also determined. The detailed work plan for fulfilling objective 3 is presented in Fig. 3.4.

3.1.18.1 Preparation of foam

Pineapple pulp was treated under cold plasma at standardized conditions optimized from objective 1 (25 kV for 15 min). The pulp was then subjected to foaming by employing a blender or food processor (Model # 2663, Usha, India). About 150 mL of pineapple pulp was taken in a mixing jar.

Apart from using CMC 0.25% and 1% starch for all trials, the quantity of SMP was varied at 2, 4, and 6%, while the whipping time (WT) was maintained at 2 min. All the ingredients were mixed, and the foaming process was done using a whipping jar. After conducting the preliminary trials, the levels of SMP were arrived at to obtain a good foam volume. After incorporating the additives, the pH of the fresh pulp and all samples were measured and found to be 3.57±0.01 and 4.69±0.02 to 5.27±0.17, respectively. All the experiments were repeated three times.

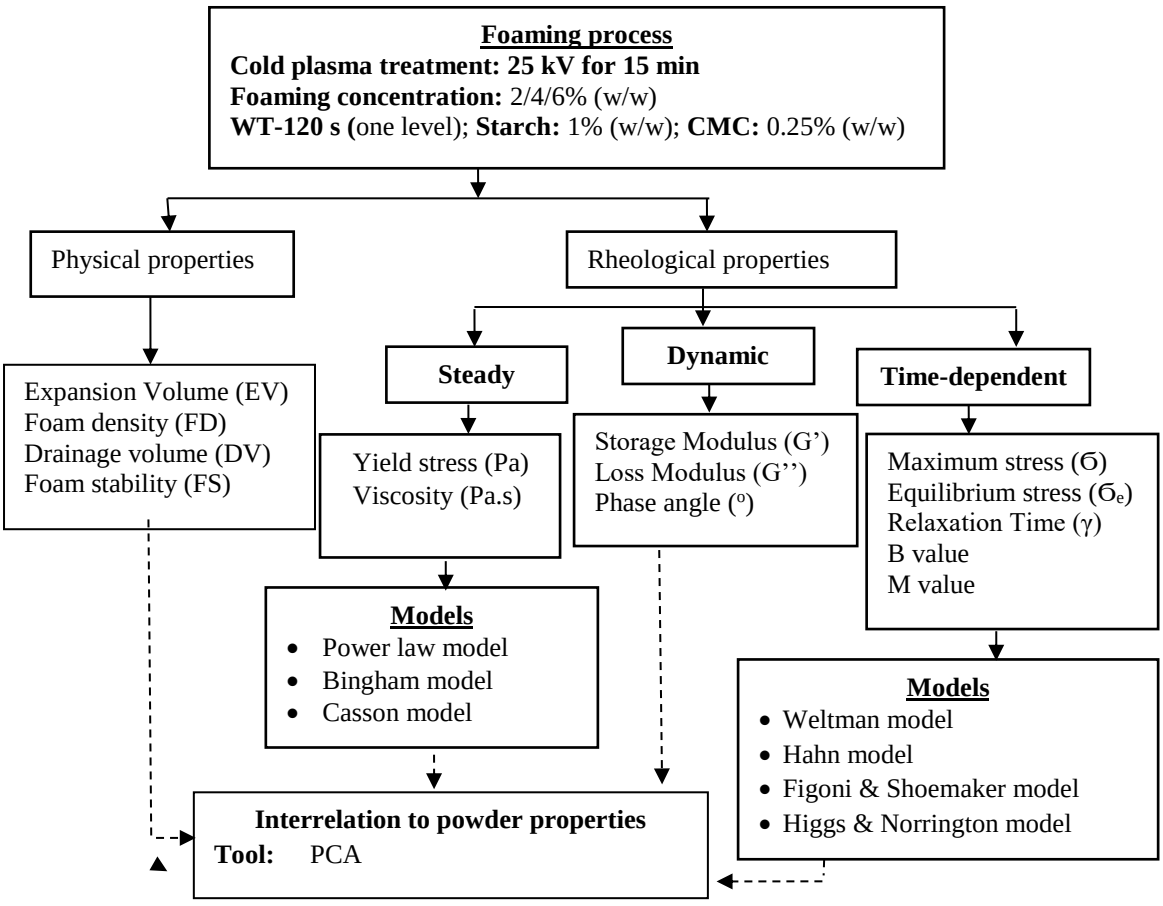

Figure 3.4 The schematic diagram of a methodology for objective #3

Experimentation conditions **Steady rheological conditions** **Shear rate**=0.1-50 s^{-1}; **Gap**=2 mm; **Temperature**=25 °C; **Plate/plate geometry** =50 mm	
Dynamic rheological conditions: **Frequency (f) =** 1-50 (Hz); **Strain**= 1% (constant); **Temperature**=25 °C	
Time-dependent conditions: **Shear rate:** 1/10/50 s^{-1}; **Time: 30** min	

3.1.19 Physical characteristics of foam

3.1.19.1 Foam expansion, stability, and drainage volume

The physical properties of the pineapple pulp foam were measured following the methods described in section 3.9.3.

3.1.20 Rheological properties of foam

3.1.20.1 Steady rheology of foam

Pineapple foam's steady shear rheological characteristics were assessed using a strain-controlled Physica MCR 72 Rheometer (Anton Paar). A plate/plate geometry (50 mm diameter, 2 mm gap) was employed at 25 ºC with a shear rate varying from 0.1 to 50 s^{-1} to acquire steady shear (shear stress and shear rate) data. The data obtained from the steady rheology has been fitted with various rheological models. The shear stresses versus shear rate data were fitted with the various rheological models, viz., Power law model (Eq. 3.23) (Karaman et al., 2015), Bingham plastic model (Eq. 3.24) (Diamante & Umemoto, 2015), and Casson model (Eq. 3.25) (Martínez-Padilla, 2024)

Power law model,	$\tau = k\gamma^n$	Eq. (3.23)
Bingham plastic model,	$\tau = \tau_o + \eta\boldsymbol{\gamma}$	Eq. (3.24)
Casson model,	$\tau^{1/2} = (\tau_c)^{1/2} + k_c(\gamma)^{1/2}$	Eq. (3.25)

Where τ, γ is the shear stress and rate, respectively. τ_o ,τ_c , η, and k_c are the Bingham and Casson yield stress and the plastic viscosity, respectively. k and n are the consistency and flow behavior index, respectively.

3.1.20.2 Dynamic rheology of foam

Dynamic rheology was employed using the method explained by Sonawane et al. (2020) on the pineapple pulp foam. The dynamic oscillation method measured the pineapple foam's dynamic rheological characteristics using a Rheometer (Anton Paar, MCR 72, Austria) (Sonawane et al., 2020; Raharitsifa et al., 2006). After the immediate preparation of foam, a small sample was poured into parallel plates (gap 2 mm) (diameter 50 mm). The extra sample was removed with a stainless-steel spatula to continue further experiments. The experiments were conducted at 25 ºC with a 1% strain (Within the linear viscoelastic region) and frequency (ω) from 1 to 50 Hz. The linear viscoelastic region of pineapple pulp

foam was determined following the method of Rubio & Rubio (2019) with a minor modification. The Dynamic moduli (G′, G″), complex viscosity (η*), phase angle (δ), and yield stress (σ_0) of the pineapple foam were determined. The phase angle and complex viscosity were determined using the following (Eqs. 3.26 and 3.27) [Patel et al., (2022); Sonawane et al., (2020)].

$$Phaseangle(\delta) = \tan^{-1}\left(\frac{G''}{G'}\right) \quad \text{Eq. (3.26)}$$

$$\text{Complex viscosity } (\eta^*) = \sqrt{\left(\frac{G'}{\omega}\right)^2 + \left(\frac{G''}{\omega}\right)^2} \quad \text{Eq. (3.27)}$$

Where G', G" are the storage and loss modulus, respectively, and ω is the angular frequency.

3.1.20.3 Time-dependent rheology of foam

The time-dependent rheological characterization of the foam was conducted by employing a controlled stress rheometer (model # MCR 72, Anton Paar, Austria). A parallel plate attachment (50 mm in diameter) was employed with maintaining a gap of 2 mm. The excess sample was trimmed off, and a metal cover was put around the sample to minimize moisture loss. After allowing the sample to relax for 10 min, it was subjected to shearing for up to 30 min for each shear rate applied, while the shear rates selected were 1, 10, and 50 s^{-1}. The temperature of measurement was maintained at 25 ^oC. All rheological measurements were repeated three times.

The experimental shear stresses versus time of shearing, obtained at individual shear rates of 1, 10, and 50 s^{-1} up to 30 min, were fitted to Weltman (Eq. 3.28), Hahn (Eq. 3.29), and Figoni and Shoemaker (Eq. 3.30) models. The best model describing the characteristics of pineapple foam was chosen with an R^2 close to 1 and the lowest error/RMSE values. The coefficients of thixotropic breakdown (B and M) were determined from Eqs. (3.31) and (3.32) and relaxation time using Eq. 3.33.

3.1.20.4 Theoretical considerations

The stability of foam is a critical criterion for developing foam-mat-dried products. The prepared foam should be stable and low-density to make drying efficient. The stability of foam may be judged in several ways. In the present study, the time-dependent characteristics of the foam have been investigated, and a disturbance in the form of shear

rate has been imposed over time. The rheological characteristics have been determined. Further, selected time-dependent rheological models have been applied, and the computed model parameters are used as indices of foam stability or foam breakdown.

Several mathematical models have described the time-dependent flow behavior of non-Newtonian fluids (Weltman, 1943; Hahn, 1959; and Figoni and Shoemaker, 1983). The structural rearrangement of the non-Newtonian fluids can be deliberated in terms of their model parameters. Shear stress against the time of shearing at a fixed shear rate has been fitted to the Weltman (Eq.3.27), Hahn (Eq.3.28), and Figoni and Shoemaker (Eq. 3.29) models to predict the time dependency of the samples and examine the suitability of these models.

$$\sigma = A_W - B_W ln(t) \quad \text{Eq. (3.28)}$$

$$ln(\sigma - \sigma_e) = A_H - B_H\,(t) \quad \text{Eq. (3.29)}$$

$$(\sigma - \sigma_e) = (\sigma_{max} - \sigma_e) exp(-A_{FS} t) \quad \text{Eq. (3.30)}$$

Here, σ indicates the shear stress (Pa), A_w is the initial stress (Pa) required for the sample to flow, B_w represents the rate of structural breakdown (both the extent of change thixotropic or equilibrium shear-stress), t is the time of shearing, and the model parameters A_H and B_H are the empirical constants of the Hahn model, σ_{max} is the maximum stress (Pa), and A_{FS} is the decay rate constant. The equations of Weltman, Hahn, and Figoni and Shoemaker are represented by Eqs. 3.28, 3.29, and 3.30, respectively.

Time-dependent fluids' thixotropic breakdown properties can be quantified using two model parameters, viz., B-value and M-value breakdown due to increasing time and shear rate, respectively (Weltman, 1943; Green & Weltman, 1943) (Eqs. 3.31 and 3.32). The t_1 and t_2 are times when the apparent viscosities are η_1 and η_2, respectively. On the other hand, η_3 and η_4 are the apparent viscosities at the rotational speeds of N_3 and N_4, respectively.

$$B = \frac{(\eta_1 - \eta_2)}{\left[ln\left(\frac{t_2}{t_1}\right)\right]} \quad \text{Eq. (3.31)}$$

$$M = \frac{2(\eta_3 - \eta_4)}{\left[ln\left(\frac{N_4}{N_3}\right)^2\right]} \quad \text{Eq. (3.32)}$$

The structure change rate over time at a fixed shear rate is represented by the parameter time coefficient (B). The loss in stress with increasing shear rate is attributed to structural breakdown, as indicated by parameter M.

The relaxation time (λ) is the parameter used to estimate the time required for the sample to relax. It is the time taken for the initial stress to decay by 1/e. Relaxation time can be calculated from the reciprocal of the slope of the plot $\ln[(\sigma-\sigma_e)/(\sigma_{max}-\sigma_e)]$ against shearing time using Eq. (3.33) (Bhattacharya, 1999).

$$ln\left[\frac{\sigma-\sigma_e}{\sigma_{max}-\sigma_e}\right]=-\frac{t}{\lambda} \qquad \text{Eq. (3.33)}$$

3.1.21 Drying of foam

The foamed pulp was poured into petri plates and dried in a tray dryer (model # NE-12, Newtech Equipment, Mumbai, India) following the methods described in section 3.9.4.

3.1.22 Quality attributes of powder

The quality attributes of powder were bulk density, porosity, rehydration ratio, flowability, dispersibility, and solubility. Quality attributes of the pineapple pulp foam dried powder were measured following the methods described in section 3.9.5.

3.1.23 Statistics and interrelation among rheological, foaming, and powder properties

The analysis concerning the rheological models was carried out employing MATLAB software. Rheological parameters with the highest correlation coefficient (r) and lowest RMSE were judged as the best-fit model. Partial component analysis (PCA) using Minitab Statistical Software (Version 20.0) was used to identify the inter-relationship among the independent and dependent parameters of the rheological, foaming, and powder properties. Pearson correlation coefficients were also determined to identify the interaction between/among variables.

3.1.24 To study the storage behaviour of pineapple pulp foam dried powder

The foam mat dried powder's storage behaviour was estimated by the gravimetric method at different relative humidity (70 to 90%) under different temperatures between 30 and 50 °C. The detailed work plan to fulfill research Objective 4 is shown in Figure 3.5.

3.1.24.1 Preparation of powder samples

Good qualities of ripened pineapples were collected from the local area of Tezpur University, Tezpur, Assam. Pineapples were then washed, cleaned with water, and cut into pieces. Pineapple pieces were ground using a home mixer grinder (Model: 2663, Usha, India) to produce smooth pineapple pulp. The pineapple pulp was foamed with SMP at a fixed concentration of 6 % and other additives (CMC-0.25% and starch-1%) and whipped for 2 min. CMC added during the foam preparation helps stabilize the foam during drying. All the chemicals used in these studies were of good analytical grade. The prepared foam was poured on a Petri plate, maintaining a thickness of 10 mm, and dried in a tray dryer (NE-12, Newtech Equipment, Mumbai, India) at a drying temperature of 60 ^{o}C. The weight loss of the samples every 30 min was recorded, and it continued till the desired moisture content of 6 % (db).

3.1.24.2 Isotherm study

Foam-mat dried powder was kept in two different kinds (PP and AL) of packaging materials and stored under three different temperature conditions of 30, 40, and 50 °C (± 1°C). Aluminium laminated packaging materials are often chosen over other materials for storing foods, especially hygroscopic materials, mainly because of their barrier properties against water vapour.

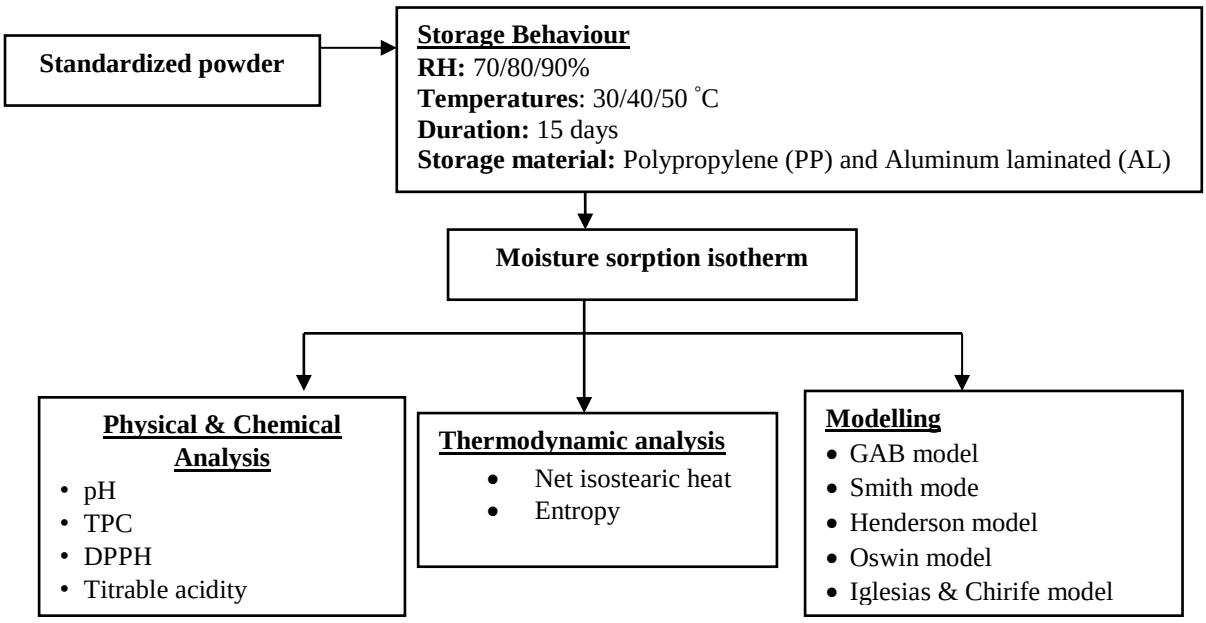

Figure 3.5 Workplan flowchart of objective # 4

The EMC of the powder was estimated under different relative humidities: 70, 80, and 90%. The relative humidity of the samples during storage was maintained by putting the samples under Different saturated salt solutions in the desiccators. The samples were then stored under different temperature-controlled cabinets, and the equilibrium condition was determined when the weight change in successive readings was less than ± 0.001g. The weight change with the storage period was noted, and their values were fitted with the different mathematical models. Samples were dried at 70 ^{o}C in a vacuum oven to obtain EMC.

3.1.24.3 Mathematical modelling of sorption isotherm

Powder samples were stored at different temperatures to generate the sorption isotherms. Various mathematical models were fitted with experimental observations to estimate the model parameters and used as indices to interpret their isothermal behaviour. GAB model (Eq. 3.34) (Van den Berg, 1984), Smith (Eq. 3.35) (Rodriguez et al., 2015), Henderson (Eq. 3.36) (Singh & Kumari, 2014), Oswin (Eq. 3.37), and Iglesias &Chirife (Eq. 3.38) (Iglesias et al., 1982) as shown below.

GAB model,	$M_e = \frac{M_G C_G K_G a_w}{(1-K_G a_w)(1-K_G a_w+C_G K_G a_w)}$	Eq. (3.34)
Smith model,	$M_e = A_S + B_S ln(1 - a_w)$	Eq. (3.35)
Henderson model,	$M_e = ln\left(\frac{1-a_W}{-A_H}\right)^{\left(1/B_H\right)}$	Eq. (3.36)
Oswin model,	$M_e = A_{OS}\left(\frac{a_W}{(1-a_W)}\right)^{B_{OS}}$	Eq. (3.37)
Iglesias and Chirife model,	$M_e = A_{IC} + B_{IC}\frac{a_w}{(1-a_w)}$	Eq. (3.38)

Where M_e is the EMC of the sample (kg/kg dry solid), M_G is the monolayer moisture content, a_w is the water activity, C_G, K_G, A_S, B_S, A_H, B_H, A_{OS}, B_{OS}, A_{IC}, and B_{IC} are the model constants, C_G and K_G signify the interaction of energies between first and further molecules at the individual sorption sites.

3.1.24.4 Thermodynamic properties of the Sorption phenomenon

Net isosteric heat (Q_{st}) of sorption is the difference between the total heat of sorption at a given system temperature in a food material and the heat of vaporization of water. This parameter (Net isosteric heat, $Q_{st,n}$) can be calculated using the Clausius-Clapeyron equation, given by:

$$\left[\frac{d(lna_w)}{d\left(\frac{1}{T}\right)}\right]_M = \frac{Q_{st,n}}{R} \quad \text{Eq. (3.39)}$$

$$Q_{st,n} = Q_{st} - \Delta H_{vap} \quad \text{Eq. (3.40)}$$

Where a_w is the water activity, T is the temperature in K, R is the constant, and its value equals 8.314 $Jmol^{-1}$ K^{-1}, and $\boldsymbol{\Delta}$H is the heat of vaporization of water in its pure state (KJ/ mol water).

The change in entropy in a material when it acts as an adsorbent or absorbent is measured by a thermodynamic property called sorption entropy ($\boldsymbol{\Delta}$S). Entropy changes in the present investigations were proposed to investigate their changes during the isotherm study of the powder. For determining the net isosteric heat ($Q_{st,n}$) and sorption entropy ($\boldsymbol{\Delta}$S), the water activity-suited predicted coefficient was selected based on the coefficient of determination and lowest RMSE (R^2 close to 1). The plots of the logarithm of the water activity were plotted against the absolute temperature (K). The changes in $Q_{st,n,}$ and $\boldsymbol{\Delta}$S were determined from the eq. 3.41. The given equation is compared with the slope obtained from (ln a_w versus 1/T), the regression line (y=mx+c), and the thermodynamic parameters were determined. The slope (Qst, n/R) of the line gives the isosteric heat ($Q_{st,\ n}$), while the sorption entropy was determined from the intercept ($\boldsymbol{\Delta}$S/R) of the regression line.

$$-lna_w = \frac{Q_{st,n}}{R} - \frac{\Delta S}{R} \quad \text{Eq. (3.41)}$$

The values of the $Q_{st,n,}$ and $\boldsymbol{\Delta}$S were obtained for each set of the experiment from Eq.3.41 and plotted Q_{st} against $\boldsymbol{\Delta}$S. Their relationship obtained from the linear regression can be correlated according to Eq. 3.42 given below:

$$\Delta H = T_B \boldsymbol{\Delta S} + \boldsymbol{\Delta G_B} \quad \text{Eq. (3.42)}$$

3.1.25 Physicochemical properties of powder during storage

3.1.25.1 Total phenolic content (TPC)

TPC of the powder samples was analyzed following the methods described in section 3.8.2.

3.1.25.2 DPPH radical scavenging activity

DPPH of the fruit juice was measured based on the scavenging effect of the DPPH free radical by using the method measured following the methods described in section 3.8.3.

3.1.25.3 pH and Acidity of powder

pH of the samples was measured as described in section 3.8.4. The pineapple pulp was subjected to proximate analysis using the AOAC (1999) method on triplicate samples. For Acidity, pineapple pulp was added with distilled water at a (10:90) ratio and then filtered. 20 ml of filtrate was added with two drops of phenolphthalein and titrated with 0.1 M NaOH. The Acidity of the sample was measured in terms of citric acid as shown below in Eq. 3.43.

$$\text{Acidity (as citric)} = V \times 7.005\text{mg}/100\text{g pulp} \qquad \text{Eq. (3.43)}$$

3.1.25.4 Q_{10} value of the powder

The Q_{10} value of the powder properties was estimated using the Arrhenius equation. The reaction rate constant against temperature was predicted using Eq. 3.2. By plotting the logarithm of reaction rates against the reciprocal of absolute temperature (1/T in Kelvin), an Arrhenius plot is obtained, and the slope of this plot provides the activation energy (Ea). The estimated Ea from the slope of the plot was used to calculate the Q10 value, which expresses the factor by which a reaction rate increases with a 10 °C rise in temperature.

3.1.25.5 Statistical analysis

The Duncan test was employed in SPSS software to check the sample changes at $p<0.05$. Mathematical modelling of the enzymes has been carried out using MATLAB software. PCA analysis was also conducted to determine the relationship between the sorption isosteric heat in Minitab Statistical Software (Version 20.0). The accuracy of the fitness and best-fitted models was selected using the equations described in section 3.1.10.

Bibliography

Akaike, H. (1973). Information theory and extension of the maximum likelihood principle. In: Proceedings of the 2nd International Symposium of Information (edited by B.N. Petrov & F. Czaki), 267–281.

Asokapandian, S., Venkatachalam, S., Swamy, G. J., & Kuppusamy, K. (2016). Optimization of foaming properties and foam mat drying of muskmelon using soy protein. *Journal of Food Process Engineering*, *39*(6), 692–701.

Association of Official Analytical Chemists. (1999). Official Methods of Analysis. AOAC, Washington, DC.

Bhattacharya, S. (1999). Yield stress and time-dependent rheological properties of mango pulp. *Journal of Food Science*, 64(6), 1029–1033.

Bhusari, S. N., Muzaffar, K., & Kumar, P. (2014). Effect of carrier agents on physical and microstructural properties of spray dried tamarind pulp powder. *Powder technology*, *266*, 354–364.

Brochier, B., Mercali, G. D., & Marczak, L. D. F. (2016). Influence of moderate electric field on inactivation kinetics of peroxidase and polyphenol oxidase and on phenolic compounds of sugarcane juice treated by ohmic heating. *LWT-Food Science and Technology*, 74, 396–403.

Chang, Y. I., & Chen, T. C. (2000). Functional and gel characteristics of liquid whole egg as affected by pH alteration. *Journal of Food Engineering*, *45*(4), 237–241.

Diamante, L. M., Ihns, R., Savage, G. P., & Vanhanen, L. (2010). A new mathematical model for thin layer drying of fruits. *International Journal of Food Science and Technology*, *45*(9), 1956-1962.

Diamante, L., & Umemoto, M. (2015). Rheological properties of fruits and vegetables: a review. *International Journal of Food Properties*, *18*(6), 1191–1210.

Figoni, P.I., & Shoemaker, C.F. (1983). Characterization of time-dependent flow properties of mayonnaise under steady shear. *Journal of Texture Studies*, 14(4), 431–442.

Grabowski, J. A., Truong, V. D., & Daubert, C. R. (2006). Spray-drying of amylase hydrolyzed sweetpotato puree and physicochemical properties of powder. *Journal of Food Science*, *71*(5), E209-E217.

Green, H., & Weltmann, R. (1943). Analysis of thixotropy of pigment-vehicle suspensions-basic principles of the hysteresis loop. *Industrial & Engineering Chemistry Analytical Edition*, *15*(3), 201–206.

Hahn, S. J., Ree, T., & Eyring, H. (1959). Flow mechanism of thixotropic substances. *Industrial & Engineering Chemistry*, *51*(7), 856–857.

Hossain, M. A., & Rahman, S. M. (2011). Total phenolics, flavonoids and antioxidant activity of tropical fruit pineapple. *Food Research International*, *44*(3), 672–676.

Iglesias, H. A., & Chirife, J. (1982). Water sorption parameters for food and food components. *Handbook of Food Isotherms*, 23–87.

Illera, A. E., Chaple, S., Sanz, M. T., Ng, S., Lu, P., Jones, J., & Bourke, P. (2019). Effect of cold plasma on polyphenol oxidase inactivation in cloudy apple juice and on the quality parameters of the juice during storage. *Food chemistry: X*, *3*, 100049.

Islam, S., Purkayastha, M. D., Saikia, S., & Tamuly, S. (2019). Augmenting the yield of polyphenols and its antioxidant activity from fresh tea leaves of Assam by response surface approach. *The Pharm Innovation Journal*, *8*(6), 560-566.

Jinapong, N., Suphantharika, M., & Jamnong, P. (2008). Production of instant soymilk powders by ultrafiltration, spray drying and fluidized bed agglomeration. *Journal of Food Engineering*, *84*(2), 194–205.

Kadam, D. M., & Balasubramanian, S. (2011). Foam mat drying of tomato juice. *Journal of Food Processing and Preservation*, *35*(4), 488–495.

Karaman, S., Yilmaz, M. T., Kayacier, A., Dogan, M., & Yetim, H. (2015). Steady shear rheological characteristics of model system meat emulsions: Power law and exponential type models to describe effect of corn oil concentration. *Journal of Food Science and Technology*, *52*(6), 3851-3858.

Kreyenschmidt, J., Hübner, A., Beierle, E., Chonsch, L., Scherer, A., & Petersen, B. (2009). Determination of the shelf life of sliced cooked ham based on the growth of lactic acid bacteria in different steps of the chain. *Journal of Applied Microbiology*, *108*(2), 510–520.

Martínez-Padilla, L. P. (2024). Rheology of liquid foods under shear flow conditions: Recently used models. *Journal of Texture Studies*, *55*(1), e12802.

Patel, G., Murakonda, S., & Dwivedi, M. (2022). Steady and dynamic shear rheology of Indian Jujube (*Ziziphus mauritiana Lam*.) fruit pulp with physiochemical, textural, and thermal properties of the fruit. *Measurement: Food*, *5*, 100023.

Planinić, M., Velić, D., Tomas, S., Bilić, M., & Bucić, A. (2005). Modelling of drying and rehydration of carrots using Peleg's model. *European Food Research and Technology*, *221*(3), 446-451.

Raharitsifa, N., Genovese, D. B., & Ratti, C. (2006). Characterization of apple juice foams for foam-mat drying prepared with egg white protein and methylcellulose. Journal *of Food Science*, *71*(3), E142-E151.

Rodríguez-Bernal, J. M., Flores-Andrade, E., Lizarazo-Morales, C., Bonilla, E., Pascual-Pineda, L. A., Gutiérrez-López, G., & Quintanilla-Carvajal, M. X. (2015). Moisture adsorption

isotherms of the borojó fruit (*Borojoa patinoi Cuatrecasas*) and gum arabic powders. *Food and Bioproducts Processing*, *94*, 187–198.

Rubio-Merino, J., & Rubio-Hernández, F. J. (2019). Activation energy for the viscoelastic flow: Analysis of the microstructure-at-rest of (water-and milk-based) fruit beverages. *Food Chemistry*, *293*, 486–490.

Singh, A. K., & Kumari, N. (2014). Moisture sorption isotherm characteristics of ground flaxseed. *Journal of Food Processing & Technology*, *5*(4), 319.

Sonawane, A., Pathak, S., & Pradhan, R. C. (2020). Effect of processing temperature on dynamic rheological properties and color degradation kinetics of bael fruit pulp. *Journal of the Science of Food and Agriculture*, *100*(15), 5596–5602.

Stoica, P., & Selen, Y. (2004). Model-order selection: a review of information criterion rules. *IEEE Signal Processing Magazine*, *21*(4), 36-47.

Terefe, N. S., Yang, Y. H., Knoerzer, K., Buckow, R., & Versteeg, C. (2010). High pressure and thermal inactivation kinetics of polyphenol oxidase and peroxidase in strawberry puree. *Innovative Food Science & Emerging Technologies*, *11*(1), 52–60.

Valdramidis, V. P., Geeraerd, A. H., & Van Impe, J. F. (2007). Stress-adaptive responses by heat under the microscope of predictive microbiology. *Journal of Applied Microbiology*, 103(5), 1922- 1930.

Van den Berg, C. (1984). Description of water activity of foods for engineering purposes by means of the GAB model of sorption. *Engineering Science in the Food Industry*, 311–321.

Weltman, R.N. (1943). Breakdown of thixotropic behavior as function of time. *Journal of Applied Physics*, 14(7), 343–350.

Zhou, K., Gui, M., Li, P., Xing, S., Cui, T., & Peng, Z. (2012). Effect of combined function of temperature and water activity on the growth of Vibrio harveyi. *Brazilian Journal of Microbiology*, *43*, 1365–1375.